Check for updates

Europe
European Chemical
Societies Publishing

Regenerated Hoof Keratin from 1-Ethyl-3-Methylimidazolium Acetate and Insights into Disulfide-Ionic Liquid Interactions from MD Simulation

Christina Apostolidou*[a, b]

Regeneration of the hoof keratin from ionic liquids was never successful in the past because the ionic liquids were not strong enough. However, this biomaterial starts to play a central role for the preparation of biofilms in the future. In the present study, hoof keratin was regenerated for the first time from an ionic liquid by experiment and characterized by FTIR spectroscopy, Differential Scanning Calorimetry (DSC) and Scanning Electron Microscopy (SEM). As 1-Ethyl-3-methylimidazolium acetate is strong enough to dissolve hooves, which have a lot of disulfide bonds, a Molecular Dynamics (MD) simulation was performed with this ionic liquid and diphenyl disulfide. The MD simulation reveals that not only the cation as postulated after experiments were carried out, but also the anion is very important for the dissolution process. This complete picture was and is not accessible via experiments and is therefore valuable for future investigations. The anion always interacts with the disulfide bond, whereas the cation prefers in some situations a strong H–O interaction with the anion. If the cations and the anions are separated from each other so that the cation can not interact with the anion, both interact with the disulfide bond. The high solvation power of this solvent is shown by the fact that the cation interacts from the left and right side and the anion from above and below the disulfide bond.

1. Introduction

Ionic liquids are of growing interest for the chemical industry as well as for researchers. They have strongly established themselves as green solvents in chemical processes. The green properties of ionic liquids include recycling,[1] low volatility[2] and low flammability.[3] Especially the first point represents a major advantage for the environment. Other important properties of ionic liquids are their high thermal stability[4] and their exceptional strong character as solvents for biomaterials.[5] All these facts reflect their popularity as green solvents for a better environment in future. One very important field in which ionic liquids play a remarkable role as a green solvent is the protein regeneration. These proteins include for example silks, collagens, cellulases, lipases and keratins.[6] The list of applications for this area is ever-growing, stressing the decisive importance for these processes. Not only the solvents are green in these processes, but the regenerated biomaterials have also a green

aspect due to the possibility of reuse. Keratin can be found in wool, horn, feathers, human hair, skin, finger nails, animal claws and hooves.[7–10] Therefore, biomaterials with keratin can be found as waste from the slaughterhouses, poultry production or from the textile industry.[11,12] Due to the tight packing of the secondary structure and especially due to the presence of disulfide bonds, it is difficult to dissolve keratin in traditional solvents and alternative solvents are necessary.[6,8,13] Famous examples of reducing agents, which are capable of reducing the disulfide bonds, are thiols.[7,14] One important advantage of thiols is that they do not lead to a change in the protein structure.[7,14] However, thiols are toxic and therefore harmful to the environment. Here, ionic liquids play with their strong ability for dissolution a very important role. These liquids can be recovered after the processing with a biomass and the pervaporation method was successfully used for [Emim][OAc].[15]

Most of the studies in which keratin is regenerated by ionic liquids investigated wool[11,16–24] and feathers.[8,25–29] A huge amount of literature can be found for these materials, reflecting the importance and interest in this field. The study of the keratin regeneration by ionic liquids started from 2005 using [Amim][Cl], $[C_4C_1Im][BF_4]$, $[C_4C_1Im][Br]$ and $[C_4C_1Im][Cl]$.[11] Especially $[C_4C_1Im][Cl]$ was successfully used for a variety of keratins like human hair,[30] chicken,[25] turkey[8] and duck feathers[28] as well as sheep[11,16–22,24,31] and goat wool.[23] [Amim][Cl] is the second most popular ionic liquid for the regeneration of these biomaterials.[8,11,17,20,23,24,28,30] Regarding the hoof keratin, Kakkar et al. performed the keratin regeneration with the aid of urea, SDS and 2-mercaptoethanol.[7] This method led to successful regeneration but includes with 2-mercaptoethanol a toxic reagent, which is also bad for the environment. Another regeneration of goat hoof keratin was again performed with

[a] C. Apostolidou
Mulliken Center for Theoretical Chemistry, Institute of Physical and Theoretical Chemistry, Rheinische Friedrich-Wilhelms-Universität Bonn, Beringstraße 4, 53115 Bonn, Germany
E-mail: capostol@thch.uni-bonn.de
[b] C. Apostolidou
Experimental work was done in: Chemical Engineering, University of KwaZulu-Natal, 238 Mazisi Kunene Rd, Glenwood, Durban 4001, South Africa

Supporting information for this article is available on the WWW under https://doi.org/10.1002/open.202000096

ChemistryOpen

Full Papers
doi.org/10.1002/open.202000096

Chemistry Europe
European Chemical
Societies Publishing

harmful reagents.[32] Although the hoof keratin is a valuable biowaste from the slaughterhouse, a dissolution process with ionic liquids is only documented once in the literature. Lovejoy et al. showed that the solubility of the pig hoof[33] in the ionic liquids [BMIM][Cl], [(C4H9)4P][Cl] and [C4MPy][Cl] only amounts 1 w(%). For this purpose, a strong dissolving ionic liquid is necessary as the hard hoof contains more disulfide bonds than wool or feathers.[6] Such a high dissolution capability was found for [Emim][OAc]. Zhang et al.[23] showed by experiments that [Emim][OAc] and also [Bmim][OAc] had the highest ability to cleave disulfide bonds. They studied the disulfide bond content of regenerated wool keratin by a solid-phase assay and found that [Emim][OAc] and also [Bmim][OAc] led to the lowest amount of disulfide bonds, which means that these ionic liquids have a high ability for the disulfide bond cleavage. Therefore, the choice of the ionic liquid [Emim][OAc] in the present study was also encouraged by this result. Liu et al.[24] performed COSMO-RS calculations with experimental verification on the dissolution of the keratin in ionic liquids. By prediction of the logarithmic activity coefficients, important results were obtained. They found that the anion plays a significant role in the dissolution process, especially the acetate anion. [Emim][OAc] also showed from their experiments the highest solubility for wool.

Hence, one aim of the present work is to investigate the dissolution of the hard biomaterial hoof, using the strong dissolving ionic liquid [Emim][OAc]. Apart from the fact that this biomaterial has not been successfully regenerated by any ionic liquid, the dissolution of the keratins in [Emim][OAc] is rare investigated, compared to other ionic liquids. [Emim][OAc] has been successfully used to dissolve wool keratin,[24] chicken feathers[29] and goat wool keratin.[23] Therefore, this study wants to clarify if this ionic liquid is strong enough to dissolve the hoof. Furthermore, the regenerated hoof keratin is characterized by DSC, SEM and FTIR spectroscopy. A second aim of this study is to investigate interactions of [Emim][OAc] with disulfide bonds via MD simulations. Especially hooves contain a lot of disulfide bonds and hence, this biomaterial is very difficult to dissolve. This was already shown in the past by using different ionic liquids.[33] Due to the fact that [Emim][OAc] is capable of dissolving and regenerating hoof keratin for the first time, this work wants to uncover the dissolution process of the hoof keratin in this ionic liquid. The MD simulation shows the characteristic properties of the ionic liquid towards the S–S bond and hence, demonstrates reasons which lead to the dissolution of the hoof keratin. Therefore, diphenyl disulfide is simulated in [Emim][OAc]. This model system is used because Baumruck et al.[34] found via experiment that [Emim][OAc] is capable of dissolving diphenyl disulfide as well as cleaving the disulfide bonds. Moreover, they observed that the cation plays the leading role in the dissolution process by cleaving the disulfide bonds. The anion abstracts in their postulated mechanism the hydrogen atom of the cation and forms the imidazolium carbene. However, it was shown in the literature that the existence of such a carbene is unlikely, from an experimental and also theoretical point of view.[35–38] Hence, the present MD simulation study uncovers the role of the cation

and especially also the role of the anion in the dissolution process with radial distribution functions (RDFs) and their orientations around the disulfide bond with the aid of snapshots and spatial distribution functions (SDFs). By employing an ionic liquid as green solvent for the keratin regeneration and studying interactions of this ionic liquid with characteristic groups of the keratin by an MD simulation, this work provides an important contribution to green chemistry.

Experimental

Materials and preparation of materials

In order to achieve a successful dissolution process, the following procedure is of crucial importance: Bovine hoof was rasped small and washed three times with distilled water. After this, it was degreased in a Sohxlet apparatus with a 1:1 mixture of dichloromethane and hexane. A similar procedure for the bovine hoof was also shown in the literature.[7] The ionic liquid [Emim][OAc] was dried for 12 hours before the dissolution process.

Dissolution and regeneration

10.5 w(%) bovine hooves were dissolved at 353 K in [Emim][OAc]. 5.85 g degreased bovine hoof was dissolved in 49.712 g ionic liquid. The temperature was set to 353 K because it was already shown in the literature that the recovery percentage of wool keratin decreased with increasing temperature.[23] Since the regenerated wool keratin from [Emim][OAc] had a low recovery percentage[23] and the hoof showed for a variety of ionic liquids very low or no dissolution,[33] the temperature was set to 353 K. Furthermore, experimental diffusion coefficients exist for this ionic liquid until 363 K. Since the MD simulation of the present work shows a good agreement with the experimental diffusion coefficients at 353 K[39] (see Supporting Information), the ionic liquid has in the MD simulation and in the experiment a similar fluidity.

The solution was stirred until an even dissolution was achieved. This occurred after 287 hours. After this, the keratin was regenerated from ethanol. The ethanol was separated by centrifugation for 10 minutes at 10,0000 rpm. In order to get rid of any ionic liquid, the regenerated keratin was washed five times with ethanol. Finally, the regenerated keratin was dried under vacuum at 323 K for 26 h. 742.95 mg were obtained, which is around 12.7 % keratin, based on the initial weight of the hoof. The yield is in the same range like the regenerated wool keratin from [Emim][OAc] in the literature.[23]

Fourier Transform Infrared spectroscopy (FTIR)

The FTIR measurement was performed on the IRPrestige-21 FTIR spectrometer, operating in the attenuated total reflection (ATR) mode with a ZnSe crystal. The FTIR spectrum was measured in the wavenumber range of 400 cm^{-1} to 4000 cm^{-1}. Furthermore, the spectrum was baseline corrected.

Differential scanning calorimetry (DSC)

The DSC measurement was performed from 30 °C to 380 °C with a ramp rate of 10 °C per minute on a DSC-60 Shimadzu device. It was measured in closed aluminum crubicles under inert gas atmosphere (nitrogen).

ChemistryOpen

Full Papers
doi.org/10.1002/open.202000096

Chemistry Europe
European Chemical
Societies Publishing

Scanning Electron Microscopy (SEM)

The morphology of the regenerated keratin was examined with a Zeiss Leo 1450 Scanning Electron Microscope (SEM) and the samples were coated with gold before the measurement.

Computational Details

Classical MD simulations of 400 ion pairs [Emim][OAc] as well as of 400 ion pairs ionic liquid with 37 molecules diphenyl disulfide (10.5 w(%)) were carried out at 353 K, using the program package LAMMPS.[40] Since the specific amount of disulfide bonds is not known from the literature and the disulfide bonds are in the MD simulation a model for the hoof, the amount of disulfide bonds corresponds the amount of the hoof from the experiment. Such an amount in the MD simulation is much more reliable than a MD simulation with only one diphenyl disulfide in the ionic liquid. The MD simulation with diphenyl disulfide was performed with a charge scaling of 0.80 for the ionic liquid, in order to account the charge transfer between the ion pairs.[36,41–43] For this charge scaling the diffusion coefficient of the pure ionic liquid is for the cation and the anion in the same order of magnitude compared to the experiment[39] and also structural features are in agreement with experiment and theory, which is shown in detail in the Supporting Information.[44] Moreover, it was shown via computations as well as via experiments that in a vacuum full charges do not describe the liquid system well.[45–48] Furthermore, the Supporting Information shows that all RDFs and SDFs of both MD simulations are converged.

All start structures were built with packmol.[49] The force field is based on the OPLS-AA force field. In the case of the cation, the Canongia Lopes and Pádua[50] force field was used and for the anion the standard OPLS-AA[51] parameters. These parameters for the cation and the anion were taken because they were successfully used to determine the structural features[44] and diffusion coefficients[44] of [Emim][OAc] as well as interactions of [Emim][OAc] with a biomaterial.[36]

For diphenyl disulfide also the OPLS-AA force field was used and parameters as well as charges were obtained from the free available LigParGen server,[52–54] which is provided by the group of Jorgensen. This server contains OPLS-AA force field parameters with 1.14*CM1A as well as 1.14*CM1A-LBCC partial atomic charges for organic molecules or ligands. The present work used 1.14*CM1A-LBCC partial atomic charges. 1.14*CM1A-LBCC partial atomic charges were used because they follow the methodology similar to that of the AM1-BCC model, which perform well for aromatic hydrocarbons.[53]

The time step of all simulations was set to 1 fs. In order avoid hotspots in the configuration, the energy of each geometry was minimized. After this, an NVT simulation was carried out for 0.5 ns with a Nose-Hoover chain thermostat (100 fs).[55–57] Subsequently, an NPT simulation was performed for 1.0 ns. Again, a Nose-Hoover chain thermostat was used (100 fs) and the Nose-Hoover barostat was set to 1 bar and 1000 fs.[55–57] After this 1.0 ns NPT simulation, the box volume was averaged over 0.5 ns NPT simulation. Having this averaged volume, it was slightly forced to this average volume, over 0.1 ns.[58] Finally, the systems were equilibrated in an NVT ensemble for 15 ns, using again a Nose-Hoover chain thermostat (100 fs).[55–57] The production runs were performed for 200 ns and all analyzes were performed from the whole trajectory with TRAVIS.[59] The snapshots were obtained with TRAVIS,[59] by analyzing the last 100 ns from the trajectory, using the first solvation shell of all RDFs and using a minimal neighbour count of one and a maximal neighbour count of three for the cation and the anion.

Force fields are often validated by properties like the densities as well as by the enthalpy of vaporization. Especially the last mentioned property is very sensitive. The equation for calculating the enthalpy of vaporization[45] is stated as follows:

$$
\begin{aligned}
\Delta h_{vap}(T,P) &= \langle h_{gas}(T)\rangle - \langle h_{liquid}(T,P)\rangle \\
&= [\langle u_{gas}(T)\rangle + RT] \\
&\quad - [\langle u_{liquid}(T,P)\rangle + Pv] \\
&\approx [\langle u_{gas}(T)\rangle + RT] - [\langle u_{liquid}(T,P)\rangle] \\
&= \Delta u_{vap}(T,P) + RT
\end{aligned} \tag{1}
$$

This equation simply describes the enthalpy of the liquid subtracted from the enthalpy of the gas phase. The gas is ideal, and Pv stands for the pressure-volume work in the liquid, which can be neglected if it is compared to the internal energies. In order to obtain the enthalpy of vaporization for one ion pair, the liquid internal energies were divided by the total number of ion pairs in the system.[45] In order to calculate the enthalpy of vaporization of the ionic liquid, an NVT simulation of one ion pair in the gas phase was performed at 298.15 K. This NVT simulation was performed for 40 ns. For the liquid phase an NPT simulation was performed for 400 ion pairs at 298.15 K like the NPT runs described before. The density of the ionic liquid at 298 K was obtained from this NPT run. Regarding diphenyl disulfide, the calculation of the enthalpy of vaporization was performed in the same way with the only difference that the simulations were performed with 37 molecules at 370 K. The density of diphenyl disulfide was obtained from an NPT run at 338.05 K because in the simulation diphenyl disulfide is used at high temperature, being therefore a liquid and not a solid. Regarding [Emim][OAc], the enthalpy of vaporization was calculated at 298.15 K, whereas this one of diphenyl disulfide was calculated at 370 K.

Concerning [Emim][OAc], no experimental value of the enthalpy of vaporization can be found in the literature, yet. The enthalpy of vaporization for this ionic liquid was calculated by Liu et al.,[60] using the General AMBER force field GAFF.[61] Their result of the enthalpy of vaporization amounts 189 kJ/mol at 300 K and the simulation of the present work leads to 178.07 kJ/mol at 298.15 K, using unscaled charges. Therefore, these results are in the same range. The simulated liquid density of [Emim][OAc], using unscaled charges, amounts 1.0884 g/cm³ at 298.15 K, which is with around 1% error in agreement with the experiment.[62] In the present work the focus relies on structural features and a well described fluidity of the liquid, by having diffusion coefficients, which are in the magnitude of order like the experiment. It was shown in the past that scaled charges reproduce the liquid system, structural features and also diffusion coefficients very well.[44,63] The enthalpy of vaporization of the MD simulation with partial charges scaled by a factor of 0.8 amounts 131.7 kJ/mol, which is close to the experimental enthalpy of vaporization for [Bmim][OAc],[64] and the liquid density amounts 1.0462 g/cm³, both at 298.15 K. The liquid density has an error of around 4.8% and the enthalpy of vaporization decreases with scaled charges. Such deviations were also described in the literature.[63,65,66] Due to the fact that there is no experimental result of the enthalpy of vaporization, this calculation helps for future investigations. In the case of diphenyl disulfide, the enthalpy of vaporization of the present MD simulation amounts 70.23 kJ/mol at 370 K, which is around 4.2% lower than the measured value of 73.3 kJ/mol by experiment.[67] The liquid density of diphenyl disulfide was obtained from a MD simulation at 338.05 K and is with 1.128 g/cm³ around 2.3% lower than the experimental density of 1.155 g/cm³[68] at 338.05 K. Hence, these results are acceptable

ChemistryOpen

Full Papers
doi.org/10.1002/open.202000096

Chemistry Europe
European Chemical
Societies Publishing

for diphenyl disulfide. The validations of the densities at 353 K for the ionic liquid are given in the Supporting Information.

2. Results and Discussion of the experiment

2.1. Hoof keratin in [Emim][OAc]

2.1.1. DSC measurement

Figure 1 shows the DSC measurement of the regenerated hoof keratin. Four characteristic thermal events take place between 132 °C and 302 °C. Therefore, this measurement provides more information than the DSC measurement until 250 °C by Kakkar et al.,[7] who obtained the regenerated hoof keratin from a non-green solvent process.

A DSC measurement somehow reflects the structural features of keratin.

One exothermic and three endothermic peaks appear. The first endothermic peak in the DSC measurement of the present work appears at 131.88 °C and corresponds to water evaporation. This peak was found in the work of Kakkar et al.[7] at 111.38 °C, which is in the same range like in the present work. The second endothermic peak at 259.17 °C describes the denaturation of the helix. This peak corresponds to the second endothermic peak in the DSC measurement of Kakkar et al.,[7] which appears at 215.76 °C. Peptide bonds are not broken during the denaturation process. The denaturation describes the interruption of interactions that make up the secondary and tertiary structure of the protein. Consequently, the α-helix is uncoiled and looses its characteristic features.[13] Then an exothermic peak appears at 271.29 °C. Such an exothermic peak is shown for example for the regenerated feather keratin at 230 °C, and Idris et al. mentioned that this peak was described in the literature as the "melt".[8,9] This thermal event describes the peptide bond degradation. In other words, the peptide bonds are broken, which form the primary structure of the protein. Finally, the disulfide bond cleavage appears at

301.56 °C. So far, this peak is also like the exothermic peak not found in the literature for the hoof keratin because it was not investigated until such high temperatures. A similar endothermic peak at 295 °C was described in the literature as a melting or decomposition peak of wool keratin fractions with high thermal stability.[69] Hence, this result fits with the aforementioned suggestion that this peak is related to the decomposition of disulfide bonds. Furthermore, the area of the aforementioned peak reflects the content of disulfide bonds in hooves.

2.1.2. FTIR spectrum

As a next step, the FTIR spectrum of the regenerated hoof keratin is shown in Figure 2.

The infrared spectrum shows characteristic absorption bands that are mainly assigned to the peptide bonds (-CO-NH). These infrared bands are known as amide I, amide II and amide III. These three bands are affected by the secondary structure of the protein. The amide I band is mainly attributed to the C=O stretching vibration. This type of vibration occurs between 1600 cm^{-1} and 1700 cm^{-1}.[19,70] The amide II band reflects the N–H bending as well as the C–H stretching vibration and typically appears between 1480 cm^{-1} and 1580 cm^{-1}.[19,70] The amide III band results from an in phase combination of C–N stretching vibration and N–H in plane bending, including contributions from C–C stretching and also C=O bending vibrations.[7,25] This band typically occurs between 1200–1300 cm^{-1}.[19,70] Finally, there is also one characteristic band between 3270–3310 cm^{-1}, which is attributed to the N–H stretching vibration of the peptide bond and is often called Amide A band.[7] Figure 2 (inset) shows that the amide I band appears at 1643 cm^{-1} with a shoulder at 1620 cm^{-1} and that the amide II band appears at 1543 cm^{-1} with a shoulder at 1520 cm^{-1}. In the past it was shown that the amide I band of the α-helix occurs at 1643 cm^{-1},[69] and the amide II band occurs between 1550 cm^{-1} and 1540 cm^{-1}.[7,70,71] In addition, it was shown in the past that β-sheet has amide I bands between
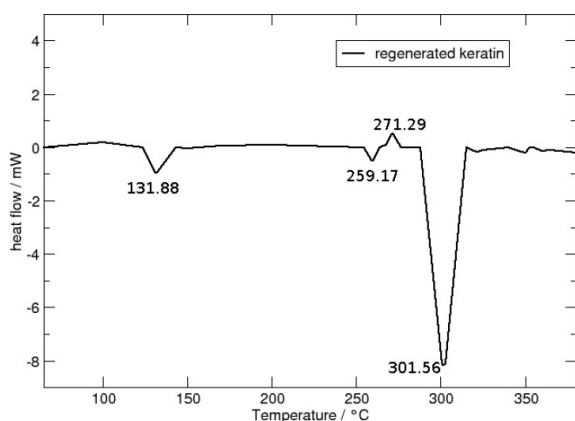
Figure 1. Differential Scanning Calorimetry (DSC) measurement of the regenerated hoof keratin with characteristic thermal events: water evaporation, denaturation of the α-helix, melting peak and cleavage of disulfide bonds (from left to right).
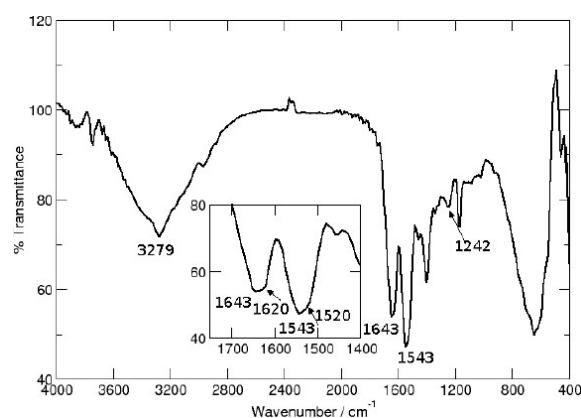
Figure 2. FTIR spectrum of the regenerated hoof keratin, showing the amide I–III bands and the hydrogen bonded N–H stretching vibration; the amide I and the amide II band of the regenerated hoof keratin are shown in the inset.

1635 cm^{-1} and 1615 cm^{-1} and amide II bands between 1535 cm^{-1} and 1520 cm^{-1}.[7,72] These results show that the regenerated material has the main peaks corresponding to the α-helical conformation and that the shoulders also suggest the presence of β-sheet conformation. The same results were also reported by Kakkar et al.,[7] also using the bovine hoof, performing the regeneration of keratin with urea, SDS and 2-mercaptoethanol. Also Vasconcelos et al.[69] found that wool treatment with formic acid increases the amount of β-sheet, which was shown by similar shoulders in the same region like in the present work. The amide III band of the present regenerated keratin appears at 1242 cm^{-1}, which fits with the above mentioned region.[19,70] Finally, the amide A band, representing the hydrogen bonded N–H stretching vibration, is found at 3279 cm^{-1}, which is in the same range like in the work by Kakkar et al.[7] In summary, the characteristic infrared bands reveal that [Emim][OAc] is able to regenerate keratin from hooves.

2.1.3. SEM measurement

Figure 3 presents the SEM image of the regenerated hoof keratin.

The image is in good agreement with the SEM images of Tran and Mututuvari for the regenerated wool keratin.[73] The regenerated hoof keratin shows a rough and porous structure, which reflects the physical properties of keratin.[73] One physical property, which was observed by both Tran and Mututuvari and during the present study, was the brittleness of this material. It was suggested that this brittleness is partially due to the porous microstructure.[73] The next section uncovers via MD simulation results reasons why the hoof, which has a huge amount of disulfide bonds, can be successfully dissolved and regenerated by [Emim][OAc], as the insolubility of the hard hoof keratin is due to the disulfide bonds.
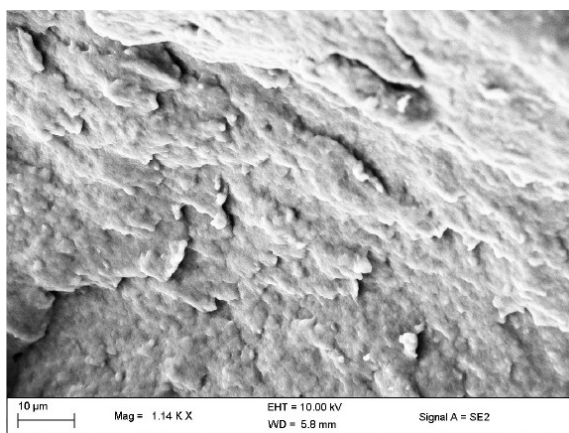
3. Results and Discussion of the MD simulations

3.1. Simulations of [Emim][OAc] with diphenyl disulfide

This section presents the results of the MD simulation with [Emim][OAc] and 10.5 w(%) diphenyl disulfide. RDFs of several interactions between the cation and the anion with diphenyl disulfide are displayed in Figure 4.

These functions show the probability of the anion or the cation at a certain distance from the disulfide bond. All interactions of the cation and the anion show oscillations at long distances, revealing weak interactions. The high probabilities for the anion and the low probabilities for the cation interactions are in agreement with the work of Zhang et al.,[23] who showed RDFs from MD simulations of cystine with [Emim][DEP] and [Bmim][Cl]. Furthermore, the anion interacts especially with its two carbon and also both oxygen atoms. These possibilities of interactions of the anion indicate that the anion helps to dissolve this hard biomaterial. Therefore, the anion also plays an important role in the dissolution process of this work. This fact was also found by COSMO-RS calculations, especially for the acetate anion.[24] The dissolution of diphenyl disulfide in [Emim][OAc] was investigated via experiment by Baumruck et al.[34] They found that the disulfide bond was cleaved by the cation. The anion abstracts in their postulated mechanism the hydrogen atom of the carbon atom between the two nitrogen atoms in the imidazolium cation, forming therefore a carbene. Gehrke et al.[36] also found via MD simulation of [Emim][OAc] with cellulose and its fragments that the anion plays a significant role for the solvent-solute interactions. This fact is interesting because Baumruck et al.[34] stressed with their experiment that only the cation plays a role by breaking the S–S bond and postulated a reaction mechanism with the aforementioned carbene, which is questionable. Regarding the carbene,
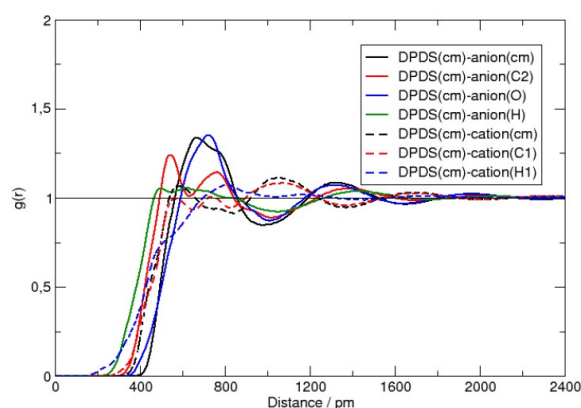
Figure 3. SEM image of the regenerated hoof keratin, revealing the rough and porous structure.

Figure 4. RDFs between the center of mass of diphenyl disulfide (DPDS) and the center of mass of the cation and the anion (carbon atom which is connected with the oxygen atoms) as well as interactions of the center of mass of DPDS with the C2 atom of the anion (methyl group), H atoms and oxygen atoms of the anion, the C1 atom of the cation (connected with both nitrogen atoms in the imidazolium ring) and the H1 atom of the cation (connected with C1); interactions of the anion are displayed with solid and those of the cation with dashed lines.

the reaction path of a reaction of [Emim][OAc] with anisalde-hyde was favoured without a carbene.[35] Furthermore, this carbene was neither observed via experiments nor supported by theoretical calculations.[37,38] This indicates that the concentration of carbenes must be low.[35] Therefore, the reaction must proceed without the formation of a carbene. With the aid of these facts and the results of the present work, it is apparent that not only the cation is responsible for the dissolution of the hoof in [Emim][OAc], but also the anion.

Figure 5 shows with the aid of SDFs how diphenyl disulfide is surrounded by the cations and the anions. In picture a the center of mass of the cation is mostly located on the right and left side of the S—S bond as well as slightly behind, in the front lower and on the top right of the S—S bond. The center of mass of the anion interacts with almost all sides from which the cation has no interaction. Therefore, interactions of the cations and the anions complement each other (picture a).

Picture c shows that the anion offers a lot of opportunities above, below, behind and in front of the disulfide bonds, being involved in the dissolution process of the hoof. These interactions are from places where the cation is not present. Therefore, it can be concluded from the pictures b and c that the anion and the cation are working together to dissolve this biomaterial.

Figure 6 shows representative simulation snapshots from the MD simulation with 400 ion pairs of [Emim][OAc] and 37 molecules of diphenyl disulfide.

Pictures a and b demonstrate that the cation and the anion have to be separated from each other because if they are on the same side, the cation prefers to interact with the oxygen atom of the anion and undergoes a weak interaction with the disulfide bond (snapshot b). The snapshot c shows that only one of the cations interacts with the disulfide bond while the other cation interacts with the oxygen atoms of both anions. This indicates that the one cation prefers the strong H—O interaction from the interaction with the disulfide bond. Such situations explain the low probability of the interaction of the cation with the disulfide bond in the RDFs. Both anions in the snapshot c interact with the disulfide bond, revealing the high probability of the anion-disulfide bond interaction in the RDFs and indicating the importance of the anion during the dissolution process. The snapshot d shows again that the separation of the cations and the anions leads to interactions of
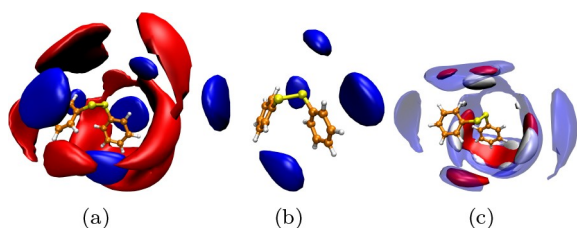

Figure 6. Representative snapshots from the MD simulation.

all cations and anions with the disulfide bond. In this case, the cation is not able to undergo the strong interaction with the oxygen atoms of the acetate anion. The next snapshot e shows a situation, which reflects the SDFs in the Figure 5 a, b and c. The two cations interact on the left and right side of the disulfide bond and the third cation interacts from behind the disulfide bond. The anions interact from above and below the disulfide bond. This snapshot uncovers that during the cleavage of the S—S bond with the cation, also the anion helps in the dissolution process with its interactions. Hence, this snapshot reflects the high solvation power of this ionic liquid, which is capable of dissolving the hoof. The last snapshot shows that two of the three cations do not interact with the disulfide bond. In contrast to this, all three anions interact and the dissolution is driven here by three anions and one cation. This snapshot highlights that the anion gives an essential contribution for the dissolution process and the disulfide bond is always solvated by the anion if the cation is not interacting with the disulfide bond.

Figure 5. SDFs of (a) the cation (blue; center of mass) and the anion (red, center of mass) (b) center of mass (blue) of the cation (c) the methyl group (grey) of the acetate, the center of mass (blue) of the acetate and the oygen atom (red) of the acetate around diphenyl disulfide in 400IL/37diph, using an isosurface of 5.
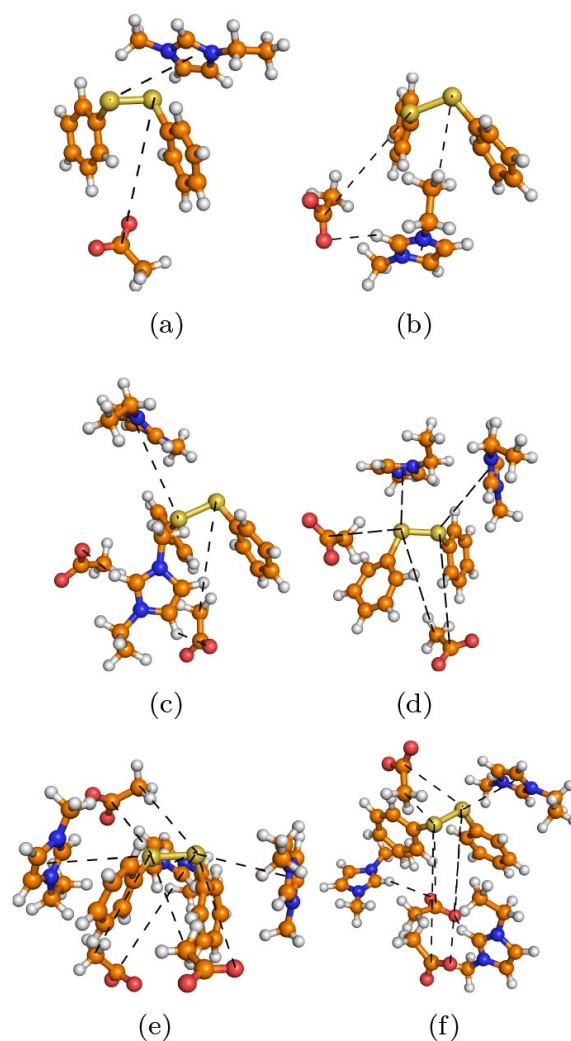
4. Conclusions

In summary, [Emim][OAc] was able to dissolve and regenerate keratin from the hoof. The regenerated keratin was successfully characterized by FTIR spectroscopy, DSC measurements and SEM. The infrared spectrum suggests beside the α-helical conformation also the presence of β-sheet conformation.[7,69] The DSC measurement reveals the characteristic thermal events including water evaporation, denaturation of the α-helix, peptide bond degradation and finally the cleavage of the disulfide bonds. The SEM measurement confirmed a porous and rough structure, reflecting the brittleness of keratin, which was also found in the past[73] and was also observed during the present work in the laboratory. Hence, the hoof is a valuable biomaterial and should be also used by industry in the future.

In order to find more about the dissolution process in this ionic liquid, an MD simulation was carried out with [Emim][OAc] and diphenyl disulfide. The aforementioned model system was used because Baumruck et al.[34] showed via experiments that [Emim][OAc] is able to cleave the disulfide bond with the aid of the cation. Therefore, diphenyl disulfide represents the disulfide bonds in the keratin and especially the hard biomaterial hoof consists a huge amount of disulfide bonds. The MD simulation shows via RDFs and SDFs that the anion plays a major role in the dissolution process and that it is able to interact from four different sides with a high probability in contrast to the cation. The low probability of the cation-disulfide bond interaction can be explained by snapshots in which the cation prefers to interact with the oxygen atoms of the anion. In such situations the anion still interacts with the disulfide bond, revealing that it is a driving force for the dissolution. Additionally, SDFs and snapshots reveal the interplay of the cation and the anion in the dissolution process. Here, the cation is mainly located on the left and right side of the disulfide bond. Having this position of the cation, the anions interact from above and below the disulfide bond, stressing that this ionic liquid has a high solvation power.

This study has a major impact on further IL applications for the hoof keratin, which should be also treated as a valuable biomaterial in the future as it is very important for biomedical applications. Recently, it was shown that on hoof keratin based biofilms contained a good antibacterial property, biocompatibility in fibroblast cell lines, cell binding as well as qualification for tissue engineering.[74] Additionally, the MD simulation uncovers insights into the interactions of the IL with the disulfide groups. These results are not available via experiment and are useful for experimenters working in the field of green chemistry, organic chemistry and bioorganic chemistry.

Acknowledgement

Conflict of Interest

The authors declare no conflict of interest.

[1] Y. Liu, A. S. Meyer, Y. Nie, S. Zhang, K. Thomsen, *Green Chem.* **2018**, *20*, 493.
[2] M. Earle, J. Esperanca, M. Gilea, J. Lopes, L. Rebelo, J. Magee, K. Seddon, J. Widegren, *Nature* **2006**, *439*, 831.
[3] D. M. Fox, J. W. Gilman, A. B. Morgan, J. R. Shields, P. H. Maupin, R. E. Lyon, H. C. D. Long, P. C. Trulove, *Ind. Eng. Chem. Res.* **2008**, *47*, 6327.
[4] W. Feng, Y. Lu, Y. Cheng, Y. Lu, T. Yang, *J. Therm. Anal. Calorim.* **2016**, *125*, 143.
[5] K. Fujita, Y. Fukuaya, H. Ohno, *Solubilization of Biomaterials into Ionic Liquids in Electrochemical Aspects of Ionic Liquids 2nd ed.*, John Wiley & Sons, **2011**, chapter 12.
[6] A. Schindl, M. L. Hagen, S. Muzammal, H. A. D. Gunasekera, A. K. Croft, *Front. Chem.* **2019**, *7*, 347.
[7] P. Kakkar, B. Madhan, G. Shanmugam, *Springerplus* **2014**, *3*, 596.
[8] A. Idris, R. Vijayaraghavan, U. A. Rana, D. Fredericks, A. F. Patti, D. R. Macfarlane, *Green Chem.* **2013**, *15*, 525.
[9] J. Cao, *Thermochim. Acta* **1999**, *335*, 5.
[10] M. Zoccola, A. Aluigi, C. Vineis, C. Tonin, F. Ferrero, M. G. Piacentino, *Biomacromolecules* **2008**, *9*, 2819.
[11] H. Xie, S. Li, S. Zhang, *Green Chem.* **2005**, *7*, 606.
[12] M. Zoccola, A. Aluigi, C. Vineis, C. Tonin, *J. Mol. Struct.* **2009**, *938*, 35.
[13] N. A. Campbell, J. B. Reece, *Biologie. sixth ed.*, Spektrum Akademischer Verlag Heidelberg - Berlin, **2003**.
[14] J. A. Maclaren, *Aust. J. Chem.* **1962**, *15*, 824.
[15] J. Sun, J. Shi, N. V. S. N. M. Konda, D. Campos, D. Liu, S. Nemser, J. Shamshina, P. Dutta, P. Berton, G. Gurau, R. D. Rogers, B. A. Simmons, S. Singh, *Biotechnol. Biofuels* **2017**, *10*, 154.
[16] N. Hameed, Q. Guo, *Carbohydr. Polym.* **2009**, *78*, 999.
[17] R. Li, D. Wang, *J. Appl. Polym. Sci.* **2013**, *127*, 2648.
[18] J. E. Plowman, S. Lee, D. P. Harland, J. M. Dyer, S. Deb-Choudhury, *Anal. Methods* **2014**, *6*, 7305.
[19] A. Ghosh, S. Clerens, S. Deb-Choudhury, J. M. Dyer, *Polym. Degrad. Stab.* **2014**, *108*, 108.
[20] A. Idris, R. Vijayaraghavan, U. A. Rana, A. F. Patti, D. R. Macfarlane, *Green Chem.* **2014**, *16*, 2857.
[21] S. Z. N. Yi, S. Zhang, X. Zhang, L. Wang, *ACS Sustainable Chem. Eng.* **2015**, *3*, 2925.
[22] C. D. Tran, F. Prosencyes, M. Franko, G. Benzi, *Carbohydr. Polym.* **2016**, *151*, 1269.
[23] Z. Zhang, Y. Nie, Q. Zhang, X. Liu, W. Tu, X. Zhang, S. Zhang, *ACS Sustainable Chem. Eng.* **2017**, *5*, 2614.
[24] X. Liu, Y. Nie, S. Zhang, A. L. Skov, *ACS Sustainable Chem. Eng.* **2018**, *6*, 17314.
[25] P. Sun, Z.-T. Liu, Z.-W. Liu, *J. Hazard. Mater.* **2009**, *170*, 786.
[26] Y.-X. Wang, X.-J. Cao, *Process Biochem.* **2012**, *47*, 896.
[27] A. Idris, R. Vijayaraghavan, A. F. Patti, D. R. Macfarlane, *ACS Sustainable Chem. Eng.* **2014**, *2*, 1888.
[28] Y. Ji, J. Chen, J. Lv, Z. Li, L. Xing, S. Ding, *Sep. Purif. Technol.* **2014**, *132*, 577.
[29] K. Kammiovirta, A.-S. Jääskeläinen, L. Kuuti, U. Holopainen-Mantila, A. Paananen, A. Suurnäkki, H. Orelma, *RSC Adv.* **2016**, *6*, 88797.
[30] M. Wang, T. Zhao, G. Wang, J. Zhou, *Text. Res. J.* **2014**, *84*, 1315.
[31] J. Chen, K. Vongsanga, X. Wang, N. Byrne, *Materials (Basel)* **2014**, *7*, 6158.
[32] S. L. Kumar, S. Anandhavelu, J. Sivaraman, M. Swathy, *Integrated Ferroelectrics* **2017**, *184*, 41.

[33] K. S. Lovejoy, A. J. Lou, L. E. Davis, T. C. Sanchez, S. Iyer, C. A. Corley, J. S. Wilkes, R. K. Feller, D. T. Fox, A. T. Koppisch, R. E. D. Sesto, *Anal. Chem.* **2012**, *84*, 9169.

[34] A. C. Baumruck, D. Tietze, A. Stark, A. A. Tietze, *J. Org. Chem.* **2017**, *82*, 7538.

[35] S. Gehrke, W. Reckien, I. Palazzo, T. Welton, O. Hollóczki, *Eur. J. Org. Chem.* **2019**, 504.

[36] S. Gehrke, K. Schmitz, O. Hollóczki, *J. Phys. Chem. B* **2017**, *121*, 4521.

[37] M. Brehm, H. Weber, A. S. Pensado, A. Stark, B. Kirchner, *Phys. Chem. Chem. Phys.* **2012**, *14*, 5030.

[38] O. Hollóczki, D. S. Firaha, J. Friedrich, M. Brehm, R. Cybik, M. Wild, A. Stark, B. Kirchner, *J. Phys. Chem. B* **2013**, *117*, 5898.

[39] R. C. Remsing, G. Hernandez, R. P. Swatlowski, W. W. Masefski, R. D. Rogers, G. Moyna, *J. Phys. Chem. B* **2008**, *112*, 11071.

[40] S. Plimpton, *J. Comp. Phys.* **1995**, *117*, 1.

[41] S. Koßmann, J. Thar, B. Kirchner, P. A. Hunt, T. Welton, *J. Chem. Phys.* **2006**, *124*, 174506.

[42] O. Hollóczki, F. Malberg, T. Welton, B. Kirchner, *Phys. Chem. Chem. Phys.* **2014**, *16*, 16880.

[43] B. Kirchner, F. Malberg, D. S. Firaha, O. Hollóczki, *J. Phys. Condens. Matter* **2015**, *27*, 463002.

[44] D. T. Bowron, C. D. Agostino, L. F. Gladden, C. Hardcare, J. D. Holbrey, M. C. Laguanas, J. McGregor, M. D. Mantle, C. L. Mullan, T. G. A. Youngs, *J. Phys. Chem. B* **2010**, *114*, 7760.

[45] K. G. Sprenger, V. W. Jaeger, J. Pfaendtner, *J. Phys. Chem. B* **2015**, *119*, 5882.

[46] Y. Zhang, E. J. Maginn, *J. Phys. Chem. B* **2012**, *116*, 10036.

[47] S. Men, K. R. J. Lovelock, P. Licence, *Phys. Chem. Chem. Phys.* **2011**, *13*, 15244.

[48] B. B. Hurisso, K. R. J. Lovelock, P. Licence, *Phys. Chem. Chem. Phys.* **2011**, *13*, 17737.

[49] L. Martinez, R. Andrade, E. G. Birgin, J. M. Martinez, *J. Comput. Chem.* **2009**, *30*, 2157.

[50] J. N. Canongia Lopes, J. Deschamps, A. A. Pádua, *J. Phys. Chem. B* **2004**, *108*, 2038.

[51] W. L. Jorgensen, D. S. Maxwell, J. Tirado-Rives, *J. Am. Chem. Soc.* **1996**, *118*, 11225.

[52] W. L. Jorgensen, J. Tirado-Rives, *J. Proc. Nat. Acad. Sci. USA* **2005**, *102*, 6665.

[53] L. S. Dodda, J. Z. Vilseck, J. Tirado-Rives, W. L. Jorgensen, *J. Phys. Chem. B* **2017**, *121*, 3864.

[54] L. S. Dodda, I. C. de Vaca, J. Tirado-Rives, W. L. Jorgensen, *Nucleic Acid Research* **2017**, *45*, W331.

[55] S. Nosé, *J. Chem. Phys.* **1984**, *81*, 511.

[56] S. Nosé, *Mol. Phys.* **1984**, *52*, 255.

[57] G. J. Martyna, M.-L. Klein, M. Tuckerman, *J. Chem. Phys.* **1992**, *97*, 2635.

[58] S. Gehrke, M. von Domaros, R. Clark, O. Hollóczki, M. Brehm, T. Welton, A. Luzar, B. Kirchner, *Faraday Discuss.* **2017**, *206*, 219.

[59] M. Brehm, B. Kirchner, *J. Chem. Inf. Model.* **2011**, *51*, 2007.

[60] H. Liu, K. L. Sale, B. M. Holmes, B. A. Simmons, S. Singh, *J. Phys. Chem. B* **2010**, *114*, 4293.

[61] J. Wang, R. M. Wolf, J. W. Caldwell, P. A. Kollman, D. A. Case, *J. Comput. Chem.* **2004**, *25*, 1157.

[62] M. G. Freire, A. R. R. Teles, M. A. A. Rocha, B. Schröder, C. M. S. S. Neves, P. J. Carvalho, D. V. Evtuguin, L. M. N. B. F. Santos, J. A. P. Coutinho, *J. Chem. Eng. Data* **2011**, *56*, 4813.

[63] M. W. Thompson, R. Matsumoto, R. L. Sacci, N. C. Sanders, P. T. Cummings, *J. Phys. Chem. B* **2019**, *123*, 1340.

[64] B. Doherty, X. Zhong, S. Gathiaka, B. Li, O. Acevedo, *J. Chem. Theory Comput.* **2017**, *13*, 6131.

[65] E. J. Maginn, *J. Phys. Condens. Matter* **2009**, *21*, 373101.

[66] M. Salanne, *Phys. Chem. Chem. Phys.* **2015**, *17*, 14270.

[67] F. Ramos, H. Flores, J. M. Hernández-Pérez, J. Sandoval-Lira, E. A. Camarillo, *J. Phys. Chem. B* **2018**, *122*, 239.

[68] *https://us.vwr.com/store/product/ 7516414/diphenyl-disulfide-99.*

[69] A. Vasconcelos, G. Freddi, A. Cavaco-Paulo, *Biomacromolecules* **2008**, *9*, 1299.

[70] E. Wojciechowska, A. Wlochowicz, A. Weelucha-Birczyńska, *J. Mol. Struct.* **2000**, *555*, 397.

[71] D. J. Lyman, J. Murray-Wijelath, M. Feughelman, *Appl. Spectrosc.* **2001**, *55*, 552.

[72] E. Goormaghtigh, J.-M. Ruysschaert, V. Raussens, *Biophys. J.* **2006**, *90*, 2946.

[73] C. D. Tran, T. M. Mututuvari, *ACS Sustainable Chem. Eng.* **2016**, *4*, 1850.

[74] S. L. Kumar, S. Anandhavelu, M. Swathy, *Integr. Ferroelectr.* **2019**, *202*, 1.